Molecular-dynamics study of displacement cascades in Cu-Au solid solutions

H. F. Deng* and D. J. Bacon
Department of Materials Science and Engineering, The University of Liverpool, Liverpool L69 3BX, United Kingdom
(Received 26 July 1995)

A molecular-dynamics study has been made of the influence of solute content on low-energy displacement cascade processes in copper containing up to 15 at. % Au in solid solution. This alloy system was chosen to illustrate the effects of heavy, oversized solute atoms in a fcc matrix. Cascades of up to 2 keV in energy were considered. The presence of the solute was found to have a significant impact on all phases of cascade development, but not on the final defect number. The ballistic phase is increased in duration, and the number of temporarily displaced atoms is increased by the solute, and the thermal spike that follows is also increased in intensity and duration. As a consequence, the atomic mixing associated with these two phases was highest in the Cu–15% Au alloy that contained the most solute. However, as a result of self-healing in the thermal spike, the final number of Frenkel defects is independent of alloy composition. To test the influence of solute atomic mass, simulations were carried out on copper containing solute atoms with the same size as Au, but a lighter mass than copper. The alloys with this fictitious element did not show the ballistic- and thermal-spike effects exhibited by those containing ''normal'' gold. The results are discussed in terms of the likely roles of solutes in damage evolution in alloys under cascade-producing irradiation.

I. INTRODUCTION

Defect production by displacement cascades is a phenomenon of major technological relevance for materials subjected to irradiation by fast atomic particles, but some of the critical issues in this production have not been recognized until recently. Computer simulation by molecular dynamics (MD) has proved to be an important technique for investigating the atomic mechanisms involved because their time and size scales are compatible with the MD method, but much too small to be open to direct experimental study. As a result of recent MD studies of metals, it has been possible to investigate aspects such as the mechanisms that lead to the eventual separation of self-interstitial atoms (SIA's) from the vacancies, the role of replacement collision sequences (RCS's) in cascade phenomena, the efficiency of defect production under cascade conditions, the clustering of both SIA's and vacancies, and cascade-induced atomic mixing in ordered alloys. By carrying out simulations on models of different metals under different conditions, the dependence of these cascade features on material, cascade energy, temperature, and crystal structure has been considered. (For reviews see Refs. 1–4.)

In the metals area, the research reported to date has been concerned mainly with fcc metals, although results from models of α-Fe (bcc) and α-Ti and α-Zr (hcp) have recently been presented. This research has increased understanding of the various collisional and thermal processes associated with cascade events and has pointed to some important characteristics of the final damage state. What is less clear is the extent to which alloying affects the cascade mechanisms. With the exception of some MD treatments of ordered alloys, little seems to have been done, despite the fact that most metals in real applications are used as alloys. Alloying is known to have important consequences for material performance in reactor cores, but the reasons are often little understood, particularly in connection with the relative contributions of possible in-cascade and post-cascade mechanisms. It is difficult to model specific alloy systems, of course, because the requirement to treat the electronic attributes of the elements in a rigorous way is beyond the scope of the interatomic potentials currently used for cascade simulation. However, it is possible to consider this problem by using models with general characteristics, with the aim of studying the influence of particular solute parameters on the cascade process, e.g., solute concentration, mass, and size. This is the approach adopted for the present work.

We have chosen copper-rich copper-gold solid solutions as a model system for investigating the effects of an oversized, heavy solute species on cascade formation in a fcc matrix. Copper has been widely used for cascade simulation by MD, and good interatomic potentials of many-body form are available for the Cu-Au system. Furthermore, by artificially reducing the atomic mass of the Au solute to a value less than that of copper, the relative effects of solute mass and size can be studied.

The influence of solutes on the various stages of cascade formation has been considered for primary–knock-on–atom (PKA) energy up to 2 keV in a matrix at 100 K using the method summarized in Sec. II. Results on the different stages of cascade evolution and the final defect state are presented in Secs. III–V, and the role of the solute in the process of atomic mixing is described in Sec. VI. It will be seen that for the most part the effects of the solute are small, except at high concentration. The implications of this in light of evidence that weak concentrations are important in some real phenomena are discussed in Sec. VII.

II. SIMULATION METHOD

The MD program used here was a version of the vectorized MOLDY code,[5] as described elsewhere,[6,7] modified to treat solid solutions of up to three atomic species. The production of a cascade was started from the energetic recoil of

TABLE I. The number of cascades simulated and the model size for the alloys and PKA energy shown.

E_p	Block size	Pure Cu	Cu–5% Au	Cu–15% Au	Cu–5% Au(lm)	Cu–15% Au(lm)
0.25 keV	4 000 atoms	12				
0.5	8 788	12				
1	16 384	8	4	4	4	4
2	32 000	4	4	4		

a single atom—the PKA—and the subsequent collisions, displacements, and recombinations of atoms with vacant sites were simulated in full detail, so that the complete structure and evolution of the cascade could be followed. The size of the MD block of atoms was chosen to avoid overlap of the cascade with itself by virtue of the periodicity. In the present work the number of atoms in a block was usually taken to be about 16 times the knock-on energy in eV, in line with the empirical relationship for adequate block size found for simulations of cascades in pure copper by Foreman *et al.*[8] For example, a block of 32 000 atoms ($20\times20\times20$ unit cells) was used to simulate displacement cascades of 2 keV, as detailed in Table I. With this choice of size, the energy imparted to the PKA results in an overall rise of 200–300 K in the temperature of the MD cell. This has little effect on the collisional and thermal spike phases of the cascade, but does assist interstitial defect migration subsequently. This is a second-order effect on defect production for the time scales considered here.

The initial lattice temperature was chosen to be 100 K for all simulations, and each block was equilibrated for at least 10 ps at 100 K before the PKA event was initiated. Each cascade for a given block corresponded to either a different equilibration time or a different PKA direction. A cascade was started by imparting a kinetic energy E_p to a PKA, and the crystallite was allowed to evolve for 600–1500 time steps (~5–12 ps) depending on the energy of the cascade. For all simulations, a high-index direction $\langle135\rangle$ was used for the PKA: this is located in the middle of the stereographic unit triangle and thus avoids channeling by the PKA. It has been found in similar modeling[6,8] that the direction of the primary recoil only affects the distance between the position of the initial PKA atom and the center of the eventual displacement cascade and has a minimal effect on the cascade shape and defect number and arrangement.

Crystalline blocks of three different compositions were modeled, namely, pure copper, Cu–5% Au and Cu–15% Au, where the compositions are in atomic percent. The latter Au level was chosen as the maximum to avoid the complication of long-range ordering. The substitutional Au atoms were generated in their initial sites in the solvent copper lattice in a random fashion. As noted in the Introduction, a series of simulations was undertaken with Au atoms of the true atomic mass of 197, which is considerably higher than the atomic mass of 63.6 of the Cu atom. As a contrast to this, to study solute mass effects alone, a corresponding series of simulations was carried out with solute atoms of a lighter mass, namely, 23, but using the same interatomic potentials. Alloys with these solutes will be labeled (lm) for ''light mass.''

We were mainly interested in the influence of solute atoms on cascade processes, and so we concentrated on E_p values for which it is believed that true cascade conditions start to apply, namely, 1 and 2 keV.[3,6,8] Since each cascade is different from any other, it is important to simulate as many cascades as possible if reasonable statistics are to be obtained and trends identified, but this aim has to be tempered by the limit imposed by computer resources when blocks of tens of thousands of atoms are employed. Sixty cascade simulations were carried out in the present work, and their distribution is detailed in Table I. The 250- and 500-eV simulations on copper were performed to examine the influence of PKA mass on low-energy cascades, and of the 12 events at each of these energy values, 6 were for a Cu PKA in pure copper and the other 6 were for a Au PKA (of normal mass 197) in otherwise pure copper; i.e., the MD block contained only one solute atom. At 1 keV, 8 cascades were simulated in copper, of which 4 were for a Cu PKA and 4 for a Au one. We were unable to detect significant differences in defect production between the cascades in copper that resulted from the two PKA species, except for the time of the collisional phase at low PKA energy,[9] and so for the 2-keV cascades in copper and all the cascades in the solid solutions of Cu-Au and Cu-Au(lm), only Cu PKA events were simulated.

The interatomic potentials used for Cu-Cu, Cu-Au, and Au-Au interactions were based on the many-body potentials of Finnis-Sinclair type derived by Ackland and Vitek,[10] but modified as described by Deng and Bacon[7] to reproduce the pressure-volume relationships of the pure metals and Cu_3Au and to provide a better treatment of interactions inside the normal nearest-neighbor distance of $a_0/\sqrt{2}$, where a_0 is the fcc lattice parameter. This modification is important for interstitial properties and the interaction of atoms in displacement events.

Point-defect properties and the displacement threshold energy E_d in dilute solutions of Au in Cu using this model were investigated by Deng and Bacon[7,9] and Bacon, Deng, and Gao.[11] Gold is an oversized substitutional solute and has a substitutional energy of -0.28 eV and a relaxation volume of $0.54\Omega_0$. The vacancy formation energy in pure copper or for a single Au solute in copper is 1.21 eV, and the formation energy of the most stable self-interstitial atom (SIA) in copper, namely, the $\langle100\rangle$ dumbbell, is 4.01 eV. The formation volume of these two defects is $0.80\Omega_0$ and $1.94\Omega_0$, respectively. The vacancy-solute and SIA-solute binding energies for the most stable pairs on nearest-neighbor sites in copper containing a single Au atom are 0.065 and 0.266 eV, respectively. As a result of the strong SIA-solute binding, the Au interstitial atom is unstable with respect to conversion to a Cu-SIA–Au substitutional pair. E_d in a copper crystal at 0 K was found to have a minimum of 20 eV for $\langle100\rangle$ orientations, 33 eV for $\langle110\rangle$, and 38 eV for $\langle111\rangle$, with a maximum of 80–90 eV around $\langle211\rangle$. These energies compare with values deduced from low-temperature electron irradia-

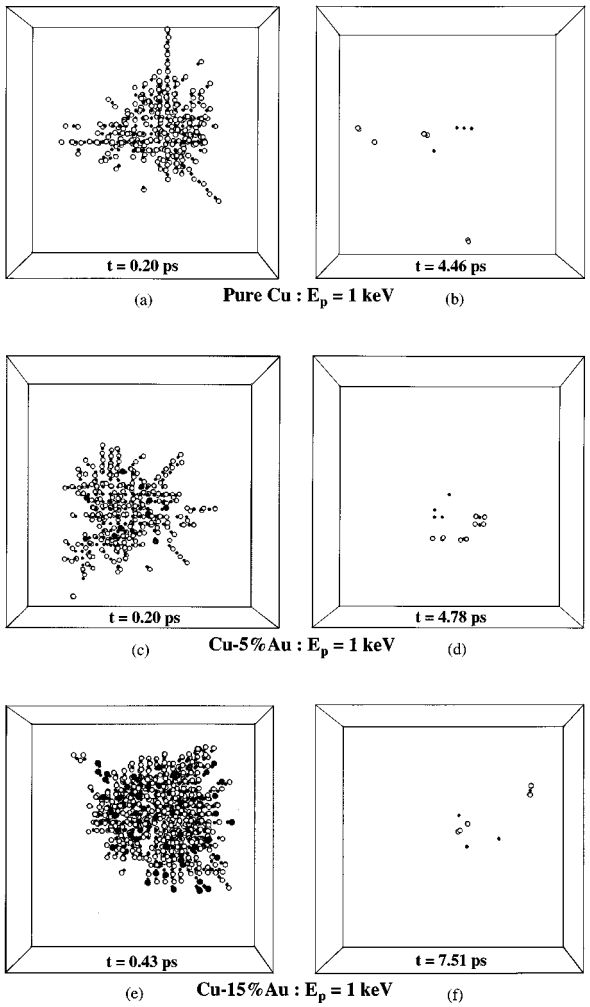

FIG. 1. Defect visualizations for 1-keV cascades in pure Cu [(a) and (b)], Cu–5% Au [(c) and (d)], and Cu–15% Au [(e) and (f)]. The figures on the left [(a), (c), (e)] are for the time t_{peak} indicated, when N_d reaches the maximum $N_d(\mathrm{max})$, and those on the right [(b), (d), (f)] are for the end of the simulation. Vacant sites are shown as small solid circles, and displaced interstitial atoms are depicted as either open circles (Cu) or shaded circles (Au). The crystal blocks are cubes of size $16a_0 \times 16a_0 \times 16a_0$.

tions by King, Merkle, and Meshii[29] of 19, 23, 76, and 79 eV, respectively. The differences may arise from features of the interatomic potential and/or the influence of temperature on collision sequences, as discussed in Ref. 7. The latter effect probably accounts for the discrepancy for $\langle 110 \rangle$ recoils. E_d for a single Au solute in otherwise pure copper is significantly less, having minima of 11 and 13 eV along $\langle 110 \rangle$ and $\langle 100 \rangle$, respectively, and a value of 22 eV along $\langle 111 \rangle$. This reduction arises because the Au atom does not easily return to its original site once it has displaced and replaced a neighboring copper atom, so that a stable Frenkel pair (involving a Cu SIA) is formed with a small vacancy-SIA separation. Thus, for example, the $\langle 110 \rangle$ threshold occurs with a RCS of only 5 replacements compared with 15 in pure copper. Similarly, the presence of a Au solute along the $\langle 110 \rangle$ row reduces E_d for a Cu atom along this direction by shortening the RCS. This suggests that such solutes may restrict the size of the displacement zone associated with cascades in metals.

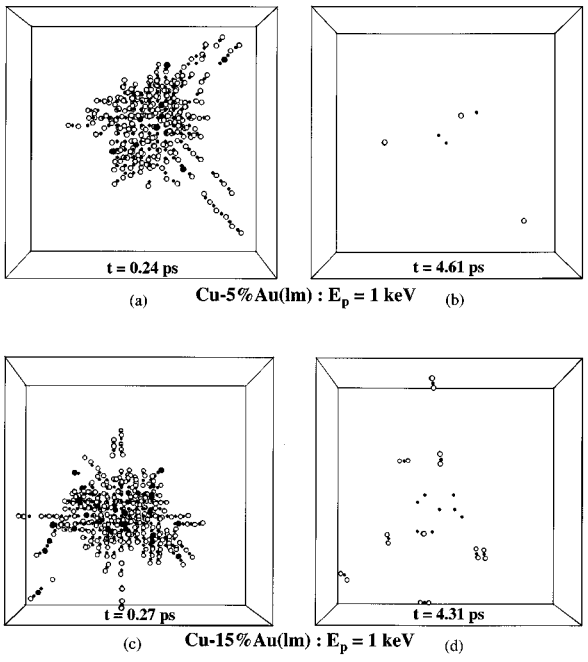

FIG. 2. Defect visualizations for 1-keV cascades in Cu–5% Au(lm) [(a) and (b)] and Cu–15% Au(lm) [(c) and (d)]. The description of these plots is as presented in the caption of Fig. 1.

III. DEFECT STATE DURING CASCADE EVOLUTION

We shall concentrate on the 1- and 2-keV cascades for the reasons stated above and will merely use the results from the 0.25- and 0.5-eV simulations[9] for analysis of final defect numbers. As expected from early ideas on cascades and recent computer studies (e.g., Ref. 3), the cascades modeled here exhibit two basic phases in their development, namely, a ballistic or collisional phase, in which the PKA initiates an avalanche of atomic displacements with a duration of a few tenths of a ps, and a relaxation or recombination phase, in which most of these displaced atoms return to empty lattice sides. The latter phase lasts a few ps, during which the thermal energy is dissipated into the surrounding lattice. Atomic movement effectively ceases (in the time scale of MD simulations) after the thermal spike has ended, and the final damage state arises from the inability of some of the displaced atoms to recombine with the vacancies.

These phases in cascade development are illustrated by the computer-generated defect plots for typical cascades in Figs. 1–3. Only ''defects,'' distinguished by size and shade, are shown in these plots. Displaced atoms are shown as interstitials (open circles for Cu, shaded circles for Au) if they do not lie within $a_0/4$ of a lattice site, and vacancies (solid circles) represent sites where no atom lies within $a_0/4$ of it. The terms ''interstitial'' and ''vacancy'' have to be interpreted with caution since most of the defects so defined exist only during the collisional and thermal spike phases, and it is only at the end of the cascade that surviving displaced atoms and empty sites represent truly stable defects. From the initial primary recoil event, there is a rapid buildup in the number N_d of displaced interstitial atoms until a maximum in this

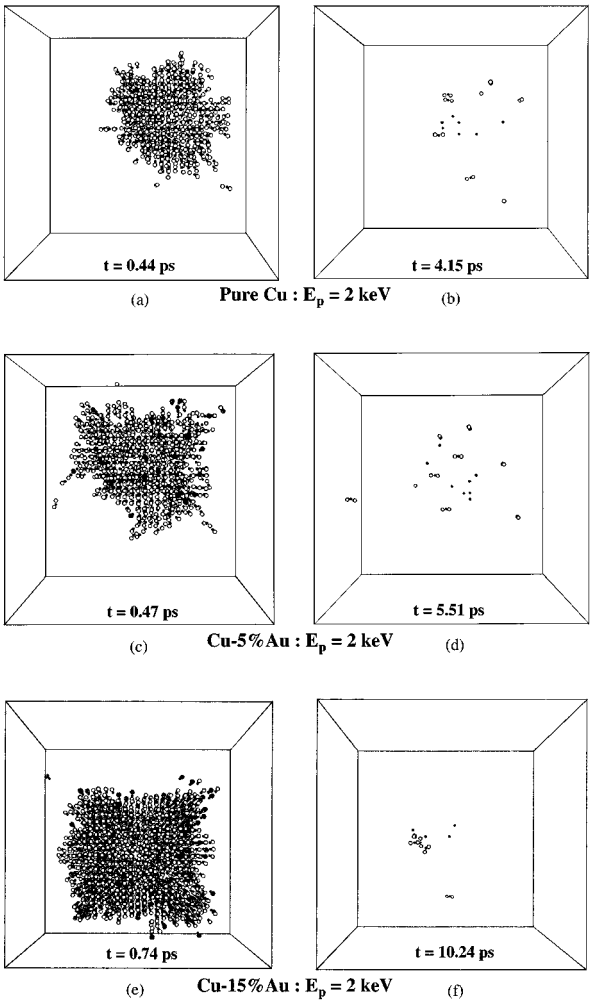

FIG. 3. Defect visualization for 2-keV cascades in pure Cu [(a) and (b)], Cu–15% Au [(c) and (d)], and Cu–15% Au [(e) and (f)]. The description of these plots is as presented in the caption of Fig. 1, except that the block size is $20a_0 \times 20a_0 \times 20a_0$.

number N_d(max) is reached. This stage occurs at a time t_{peak}, which is typically a few tenths of a ps. The defect plots on the left are for this time [i.e., parts (a), (c), and (e) of Figs. 1 and 3 and parts (a) and (c) of Fig. 2].

The effect of increasing the cascade energy at a particular Au concentration is as anticipated from other simulation studies of copper and other metals,[2,3,8] namely, an increase in the number of displaced atoms and a transition from a relatively dispersed arrangement of defects to a dense morphology between 1 and 2 keV. Individual focused collision sequences (FCS's) play a stronger part in pure copper at the lower energy. The influence of the Au concentration on the cascade morphology during the ballistic phase can be seen by comparing the plots within each figure. For this, the effect is striking. At each energy, adding the heavy, oversized solute increases the number of atoms displaced during the ballistic phase. Although the size of the damage zone also increases, the effect of the Au solute is to produce a region with a high concentration of displaced atoms. Another aspect of this is that the relative importance of individual FCS's declines sharply. The compact form of the 2-keV zone in the 15% Au alloy [Fig. 3(e)] illustrates these features very

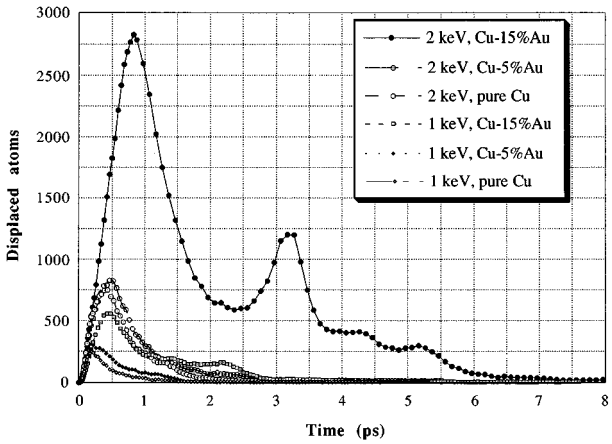

FIG. 4. Variation of the number N_d of displaced ''interstitial'' atoms with time for typical 1- and 2-keV cascades in Cu, Cu–5% Au, and Cu–15% Au.

clearly. All the plots are views of the MD cell along a ⟨100⟩ direction, and they demonstrate the increasingly collective nature of the displacement of large numbers of atoms along the close-packed ⟨110⟩ directions during the ballistic phase as either the PKA energy or the Au level increases. Finally, the effects of solute mass on the damage zone formed in the ballistic phase of 1-keV cascades can be judged from a comparison of the plots in Figs. 1 and 2 for alloys containing Au and Au(lm), respectively. There is no discernible difference between the Au(lm) alloys and pure copper in these individual cascades. For example, focused collision sequences are disrupted far less by the light mass solute than the normal mass solute. Thus the effects of Au reported above are due principally to solute mass rather than size.

During the subsequent relaxation phase of cascade evolution after the time t_{peak}, recovery due to defect recombination occurs, so that by about 1 ps most displaced atoms become reassociated with lattice sites. Shortly after that, a stable state is reached, wherein only occasional interstitial rotation and migration occurs in what is essentially a cold lattice. The variation in the number of displaced interstitial atoms, N_d, during the lifetime of the cascades in Figs. 1 and 3 is shown in Fig. 4. This demonstrates clearly the influence of Au concentration at a given E_p and of E_p at a given concentration on the zone of damage during the ballistic and thermal spike phases. First, N_d(max) increases very strongly with increasing Au solute content at both cascade energies, but particularly at 2 keV, where it increases by a factor of 4 between pure copper and the Cu–15% Au alloy. Second, the time t_{peak} to reach this maximum increases in a similar fashion. The dependence on E_p is not unexpected and is consistent with computer simulation of cascades in pure metals (e.g., Refs. 3,6).

The totality of results for N_d(max) is presented in Figs. 5(a) and 5(b), where the mean values and standard deviations are plotted as a function of E_p and Au concentration for all the simulations. These show clearly that in the ballistic phase (i) there is no discernible difference between low-energy cascades initiated by Cu and Au PKA's, (ii) the effect of small concentrations of solute of light mass on cascades at 1 keV is

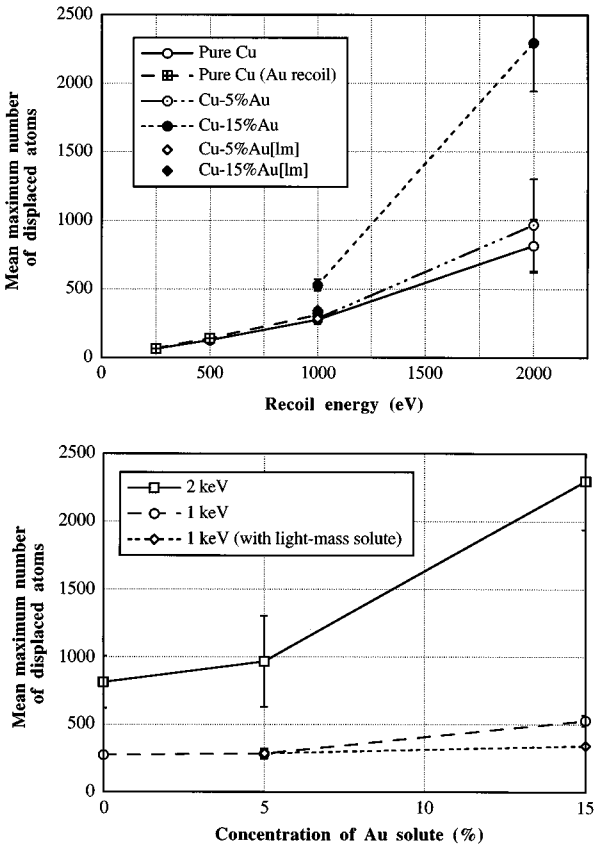

FIG. 5. Variation of the maximum number N_d(max) of displaced atoms with either (a) E_p or (b) solute concentration. The data are averaged over all the cascades at each condition.

negligible, and (iii) the strong influence of heavy Au solutes, observed above for one cascade (Fig. 4), is statistically significant. Similar conclusions can be drawn from the data plotted in Fig. 6, which shows the mean value of t_{peak} as a function of the concentration, mass, and energy variables. The large value of almost 0.8 ps for 2-keV cascades in Cu–15% Au reflects the time taken to displace the larger number

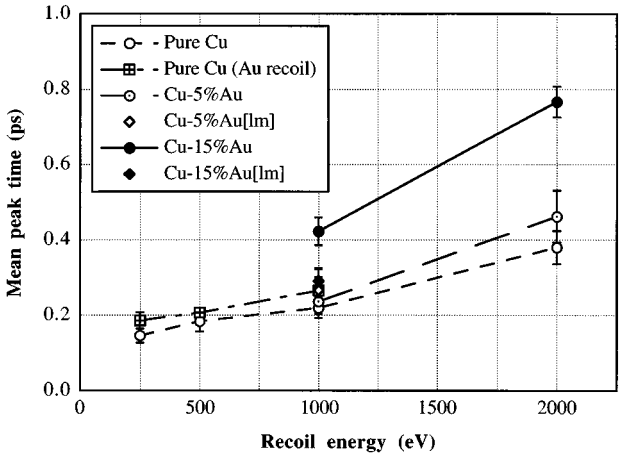

FIG. 6. Variation of the time t_{peak}, at which the number of displaced atoms reaches its maximum N_d(max), with E_p. The data are averaged over all cascades at each condition.

of atoms in cascades in this alloy. We observed that if the displaced Cu and Au atoms are analyzed separately in the alloys, t_{peak} for Au tends to be higher in some of the simulations for the Cu-Au system, but not in the Cu-Au(lm) cases. This presumably arises from an inertia effect associated with the heavier mass of the solute atoms in the former alloy.

There are two additional features revealed by Fig. 4. First, the relaxation-thermal spike phase that follows t_{peak} is greatly enhanced by increasing concentration of Au. The initial decline in N_d after t_{peak} follows the exponential decay observed in cascade simulation in pure metals and ordered alloys,[6,12,13] with a relaxation time of approximately 0.4 ps at 1 and 2 keV, independent of alloy concentration. This is associated with the return to nearby lattice sites of the majority of atoms displaced collectively in the ballistic ejection process that leads to the state seen on the left in Figs. 1–3. However, the lifetime of the atomic disturbance that follows this relaxation is strongly affected by the gold solute at both energies.

The second striking feature of the plot for the 2-keV cascade in Cu–15% Au in Fig. 4 is the second maximum in N_d just after 3 ps. This occurred to varying degrees in all the cascades at this condition and can be seen in weaker form at 1 keV and in the Cu–5% Au cases. A similar phenomenon has also been found in simulations of overlapping cascades in the ordered alloy Ni_3Al.[14] It is not a computational artifact, such as reentry of shock waves through the periodic boundaries, since it is independent of block size and occurs in Ni_3Al even when the boundary atoms are damped. It is probably associated with a thermomechanical instability in the highly disordered cascade core under conditions where the surrounding alloy prevents the rapid removal of heat by the ionic system. This region, develops liquidlike character as the cascade energy increases through the range 1–2 keV (see the review in Ref. 3) and the secondary peaks in N_d could be a reaction to pressure brought on this hot zone by the compressive relaxation of the surrounding region of displaced atoms. We suppose that the density increase in the hot core due to this effect occurs more rapidly than the loss of heat into the surrounding matrix, resulting in a compressed region of very high energy density. However, we have not investigated this effect in detail and it is not obvious that it influences the final cascade form.

IV. THERMAL SPIKE

The atomic kinetic energy was analyzed during cascade simulation, and the number of atoms with an energy greater than $3kT_m/2$ was recorded, where k is Boltzmann's constant and T_m is the melting temperature of copper. (T_m for our model is about 1250 K,[15] which is close to the true value of 1357 K.) This is a more suitable parameter to compute for the purposes of comparing different cascades than, say, the melt zone volume, which is difficult to define unambiguously.

This number is plotted as a function of time for typical cascades in each alloy in Figs. 7(a) and 7(b) for 1- and 2-keV cascades, respectively. For 1-keV cascades, the number reaches a maximum about 0.2–0.4 ps after the primary recoil event, consistent with the time t_{peak} for the maximum in the

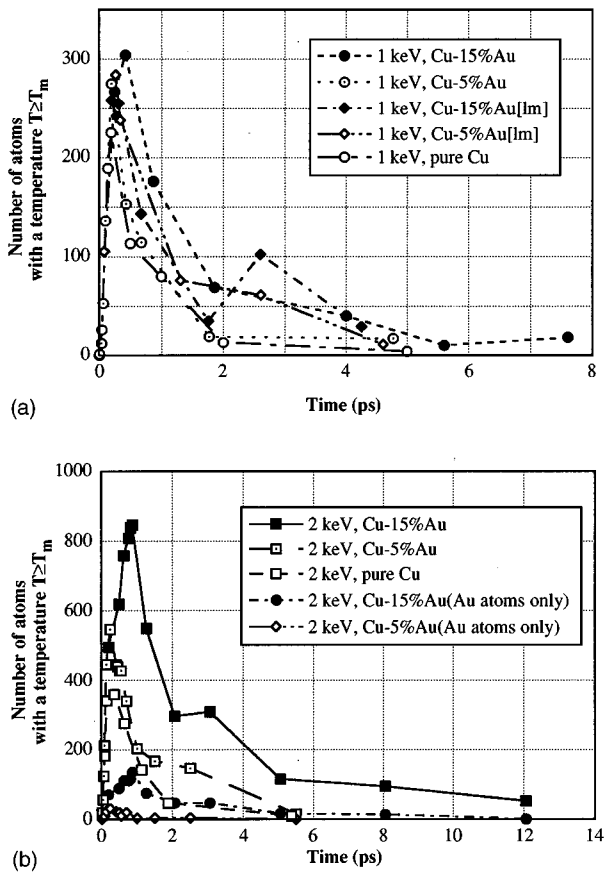

FIG. 7. Number of atoms with kinetic energy greater than $3kT_m/2$ as a function of time for typical cascades with E_p equal to either (a) 1 keV or (b) 2 keV.

number of displaced atoms reported in Fig. 6, and the peak number between 220 and 300 atoms is not sensitive to the alloy concentration or solute mass. Only the Cu–15% Au alloy stands out as having a slightly more intense and longer-lived thermal spike, as measured by this criterion. For the 2-keV cascades in copper and the two Cu-Au alloys in Fig. 7(b), there is a much stronger dependence on alloy composition. Again, the maximum in the plots is achieved at times close to t_{peak}, and at this higher cascade energy the maximum number increases significantly with increasing level of gold. Furthermore, the lifetime of the thermal spike, as measured by the number of ''hot'' atoms at times well beyond t_{peak}, also increases markedly with increasing Au content. In the 15% Au case, for example, the period for the number of atoms to decline to $1/e$ of its maximum is about 2 ps, compared to about 1 ps for the 5% Au alloy. This energy is distributed among the two elemental species in proportion to the alloy composition, as can be seen from the separate data for the gold atoms for the 2-keV cascades in Fig. 7(b): The numbers are roughly 15% and 5% of the total over most of the cascade period.

V. DEFECTS IN THE FINAL CASCADE STATE

The N_d versus time plots in Fig. 4 show that nearly all the atoms displaced in the ballistic phase return to lattice sites during the subsequent relaxation and thermal spike phases, so that at the final time t_{final} the number of defects that remains is small. From the point of view of evolution of microstructure in irradiated materials, it is this ''primary state'' of damage that matters. The defect images plotted on the right [i.e., parts (b), (d), and (f)] of Figs. 1–3 are for this time, and as in Sec. III, comparisons between the different figures can be made to provide qualitative evidence for the influence of alloy composition, solute mass, and PKA energy.

It is clear that the effects of the Au solutes, though strong in the ballistic and thermal spike phases, do not persist through to the final state at either 1 or 2 keV. To all intents and purposes, there is no difference between either the cascade in Fig. 1(b) and those in Figs. 1(d) and 1(f), or that in Fig. 3(b) and those in Figs. 3(d) and 3(f). Similarly, there is no apparent difference between the plots in Figs. 2(b) and 2(d) for the alloys with the Au(lm) solute and those for copper and Cu-Au alloys at the same energy in Fig. 1. The differences that are seen among these plots are the natural variations that occur from cascade to cascade at the same energy. As found in the simulations of pure copper by Foreman *et al.*,[8] most focused collision sequences do not result in SIA creation by the RCS mechanism and RCS events play only a small part in defect production. The second point to note is that no Au interstitials were created in any of the 60 cascades studied, for all either recombined with vacancies or converted to substitutional atoms and Cu interstitials during the thermal spike. This is consistent with the point defect energies quoted in Sec. II and is not a mass effect, but simply arises because of the oversized nature of the Au solute atom in copper.

Some of the Cu interstitials seen at t_{final} in Figs. 1–3 are the stable $\langle 100 \rangle$ dumbbell defects, and others appear to have a different form. This is because the crystal has not been quenched and is actually at a few hundred degrees, due to the absence of heat extraction in the model, and during the resulting atomic movement some atoms cross the dividing line of $a_0/4$ between interstitial atom and vacant site. In counting these various forms for statistical purposes, each was classified simply as one interstitial. The mean number of Frenkel pairs for each energy and alloy condition is plotted as a function of E_p and solute concentration in Figs. 8(a) and 8(b). The data for all energy values in Fig. 8(a) exhibit the expected increase with increasing energy and show that, within the scatter of the data, the final defect condition in the low-energy (0.25- and 0.5-keV) cascades in copper is not dependent on the change of PKA from Cu to Au. The same result was also found to apply at 1 keV. There is no clear influence of solute mass or solute concentration on the final number of Frenkel pairs at the energies of 1 and 2 keV for which true cascade conditions are believed to apply. This is demonstrated in greater clarity by the plots in Fig. 8(b). Within the statistical spread, the higher number of defects in the alloys compared with pure copper for the 2-keV cascades may not be significant.

In addition to the final number of Frenkel pairs, another factor which has come to assume importance in the modeling of radiation damage is the extent of SIA clustering.[16,17] We have therefore analyzed all the cascades to ascertain the extent of this clustering. All interstitials that had at least one nearest-neighbor interstitial in the final state were counted.

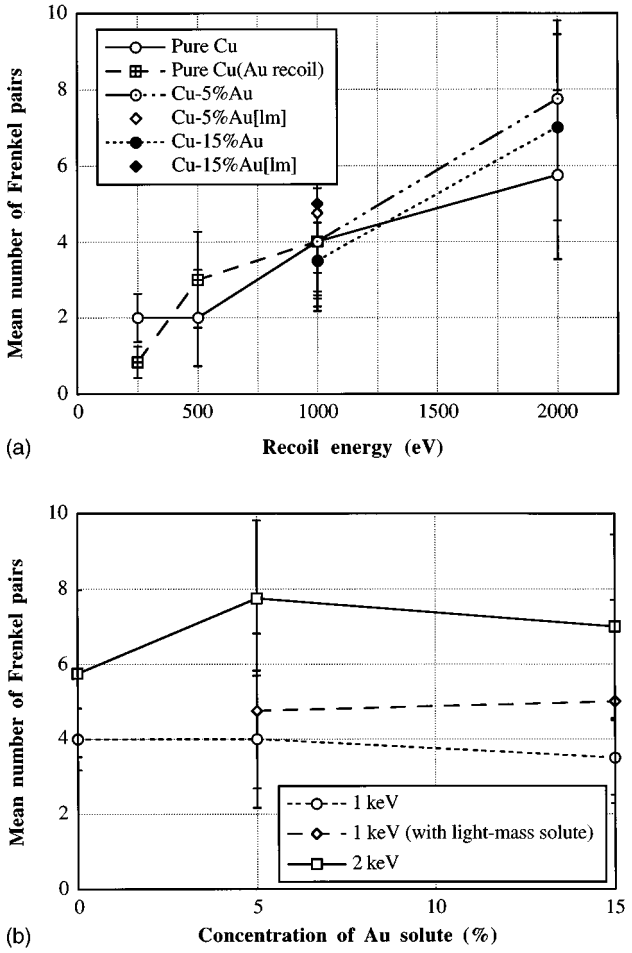

FIG. 8. Variation of the final number of Frenkel pairs with either (a) E_p or (b) solute concentration. The data are averaged over all cascades at each condition.

The results are summarized in Table II, where the mean number of single $(1i)$ and multiple (ni) interstitials per cascade in each alloy at 1 and 2 keV is given. It can be seen that the extent of clustering at 1 keV is small and not influenced by alloy content, for the $5i$ cluster created in a cascade in the Cu–15% Au(lm) alloy was the only cluster larger than a di-interstitial at this energy. The degree of clustering for the 2-keV simulations is also small, and we cannot be confident that the three higher-order clusters found in the Cu–15% Au alloy are statistically significant. On the assumption that alloy composition has no significant influence on cluster numbers, we give the mean for all cascades at each energy at the foot of the columns in the table.

VI. ATOMIC DISPLACEMENTS AND MIXING

The extent to which atoms return to sites other than their original ones after the ballistic phase is an important aspect of cascade damage because it produces the atomic mixing that accompanies irradiation of materials. We have therefore analyzed the displacement of both the solvent and solute atoms as functions of the cascade energy and alloy concentration. The distribution of displacements of the atoms from their original lattice sites in the MD cell was determined as a function of time for all the cascades simulated. Results for the distribution at the times t_{peak} and t_{final} for a typical 2-keV cascade in the alloy Cu–15% Au are shown in Fig. 9(a). The displacement is measured in units of the lattice parameter a_0, and the bin size used for the distribution is $0.1a_0$. (The point at $0.8a_0$, for instance, is the number for the range $0.7a_0 \leqslant r < 0.8a_0$. The radii of the first four neighbor shells in the fcc lattice are $0.707a_0$, $1.0a_0$, and $1.225a_0$, and $1.414a_0$ and fall at points $0.8a_0$, $1.1a_0$, $1.3a_0$, and $1.5a_0$, respectively.)

At t_{peak}, most of the atoms in the damage zone were displaced into interstitial-like positions next to their starting site, corresponding to the defect states presented in the plot in Fig. 3(e), for example, and fewer than 5% moved as far as the first-neighbor shell or beyond. A very small number moved over several lattice parameter distances as a result of channeling of energetic recoils. The separate plot for the Au solute atoms alone shows that their number distribution over most of the range is proportional to their concentration in the alloy, except for the larger movements, which these oversized solutes were unable to make. By the end of the cascade process, corresponding to the defect plot in Fig. 3(f), approximately 500 of the 2400 atoms displaced at t_{peak} were found to be displaced into nearest-neighbor sites and a further 300 atoms in total were displaced to more distant positions. Again, the Au atoms contribute proportionally to this distribution, except at the larger distances.

The other two parts of Fig. 9 compare the distribution of displacement at the final time with alloy content for typical 2-keV cascades [Fig. 9(b)] and 1-keV cascades [Fig. 9(c)]. Figure 9(b) shows that considerably more movement was produced in the 15% Au alloy than in the pure copper and 5% alloy at 2 keV, and the displacement to the second- and higher-order sites was more than doubled. A similar effect

TABLE II. Mean number of single (i) and multiple (ni) interstitials per cascade in the final state.

Material	$E_p=1$ keV					$E_i=2$ keV				
	$1i$	$2i$	$3i$	$4i$	$5i$	$1i$	$2i$	$3i$	$4i$	$5i$
Cu	2.25	0.88				3.75	0.50		0.25	
Cu–5% Au	2.50	0.75				6.25	0.75			
Cu–15% Au	2.00	0.75				2.75	0.50		0.50	0.25
Cu–5% Au(lm)	2.50	0.50			0.25					
Cu–15% Au(lm)	3.50	0.75								
Mean	2.50	0.75			0.04	4.25	0.58		0.25	0.08

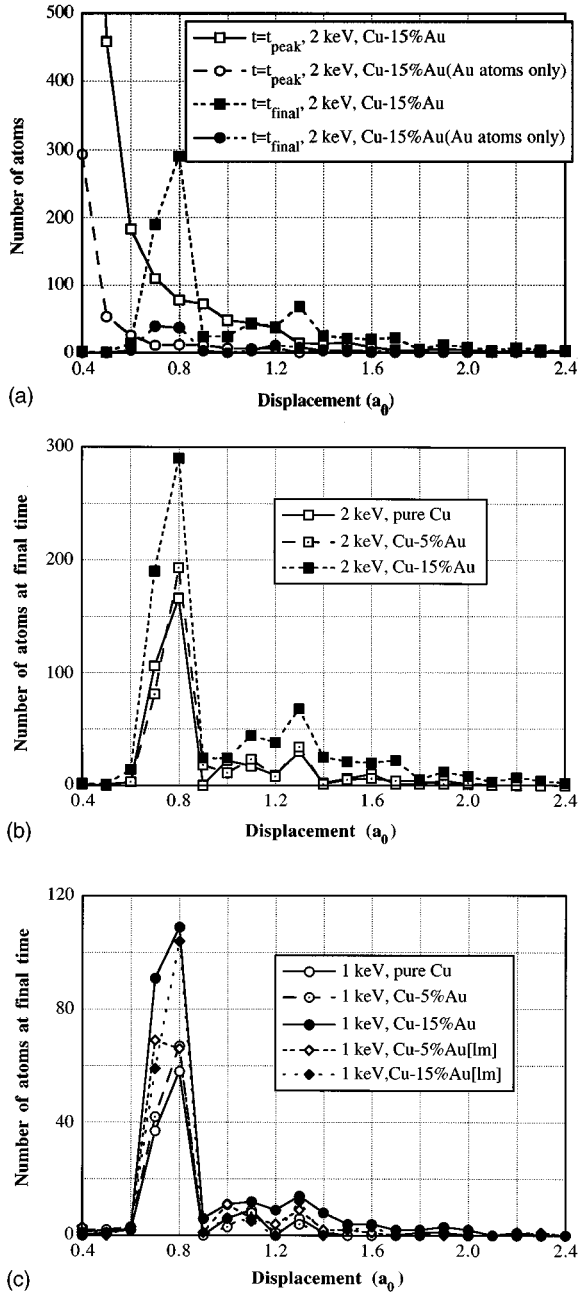

FIG. 9. Distribution of the displacement of atoms from their original position for typical cascades. (a) is for a 2-keV cascade in Cu–15% Au at the times t_{peak} and t_{final}. (b) and (c) are for t_{final} for 2- and 1-keV cascades, respectively, in all the alloys.

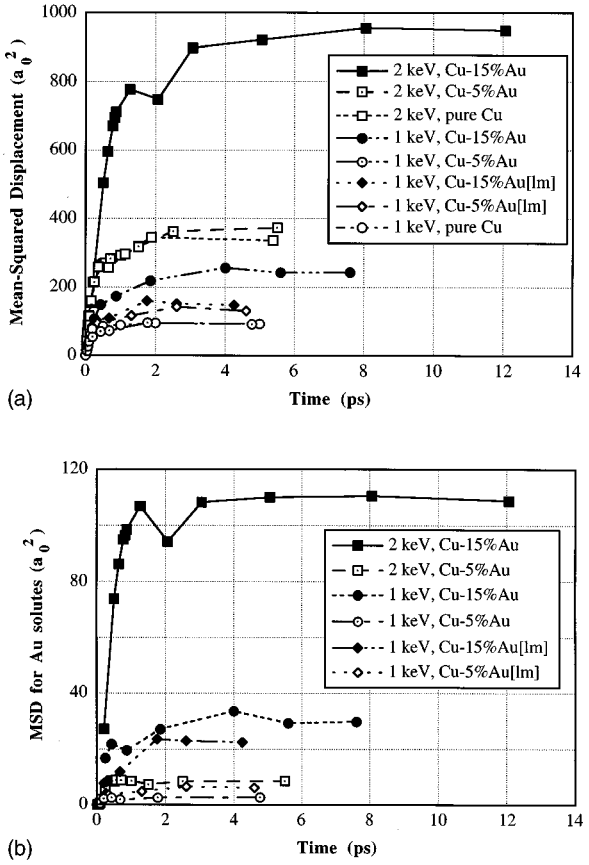

FIG. 10. Variation of the total mean-square displacement [Eq. (1)] with time for typical cascades at all conditions for (a) all atoms and (b) Au atoms only.

can be seen to have occurred at 1 keV in Fig. 9(c). The data for the alloy containing the light-mass solute in this figure exhibit a contrast to this effect, however. In this case, although the number of atoms displaced to the nearest-neighbor positions for Au(lm) is similar to that for normal Au, the numbers at the larger displacement distances are smaller for the light mass, implying that solute mass has an effect on the overall movement of solute atoms in cascades.

In terms of the atomic mixing in cascades, it is the overall displacement that is of concern, because the mean-square displacement (MSD) of the atoms can be related to an effective diffusion coefficient by the usual relation, and this in turn can be related to the mixing efficiency associated with cascade damage.[1,18,19] The MSD is obtained by comparing the instantaneous coordinates of all the atoms in the computational cell with their original ones and identifying those atoms that have moved by at least one atomic jump to other sites. (This requires that atoms that have moved beyond the Wigner-Seitz radius of $0.39a_0$ are identified with the new site to which they are closest.) The total MSD of the atoms at time t is given by

$$\langle \Delta x^2(t) \rangle = \sum_{i=1}^{N_j} |\mathbf{x}_i(t) - \mathbf{x}_i(0)|^2, \tag{1}$$

where $\mathbf{x}_i$ is the position vector of atom i and the sum is over all the atoms, N_j, that have moved to new sites at that time.

The MSD (in units of a_0^2) is shown as a function of time for a representative selection of cascades in Fig. 10(a) for all atoms and Fig. 10(b) for the solute atoms. It can be seen that $\langle \Delta x^2(t) \rangle$ rises sharply during the ballistic phase of cascade development, and thereafter it rises more gradually during the relaxation and thermal spike phases to reach a constant value. This form is the same as that observed for simulations of pure metals (e.g., Refs. 1,13,18) and ordered alloys.[12,20] The value of $\langle \Delta x^2(t) \rangle$ is seen to more than double as the cascade energy increases from 1 to 2 keV for a given alloy condition and to be strongly influenced by the presence of

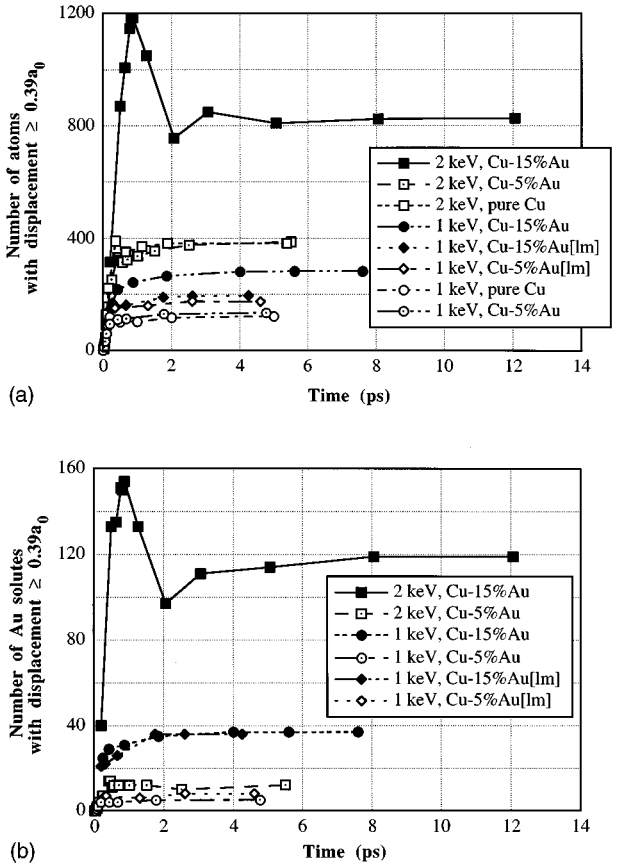

FIG. 11. Number N_j of atoms that contribute to the data in Figs. 10(a) and 10(b) are plotted in parts (a) and (b), respectively.

the Au solute at the higher concentration. Thus the MSD increases by a factor of almost 3 between pure copper and the Cu–15% Au alloy at both energies. The effect of the Au(lm) light solute at 1 keV is less severe. Figure 10(b) shows that the contribution made by the Au atoms alone to the MSD is slightly smaller than their composition fraction, being closer to 12% than 15% for the most concentrated alloy, for example.

The number of atoms, N_j, that contribute to the MSD in Figs. 10(a) and 10(b) is plotted for all atoms and the solute atoms alone in Figs. 11(a) and 11(b), respectively. These reveal that the proportion of N_j due to the Au atoms is very close to their atom fraction, and hence the smaller proportion they contribute to the MSD arises from a smaller displacement per atom for Au than Cu. This stems from the fact that very few Au atoms move beyond the nearest-neighbor step [Fig. 9(a)]. This is a consequence of their mass rather than size, as can be verified from the data for the alloys containing the Au(lm) solute. It can also be seen that the final value of N_j for the 2-keV cascade in the 15% Au alloy is less by about 30% than its value at the end of the ballistic phase, whereas the MSD itself does not exhibit this effect. This shows that the MSD per atom increases from about $0.59a_0^2$ to $1.16a_0^2$ after the end of this phase, presumably as a result of the high energy density and long lifetime of the thermal spike in this alloy. In pure copper at the same cascade energy, the MSD per atom only increases from $0.66a_0^2$ to $0.86a_0^2$ during the relaxation and thermal phases.

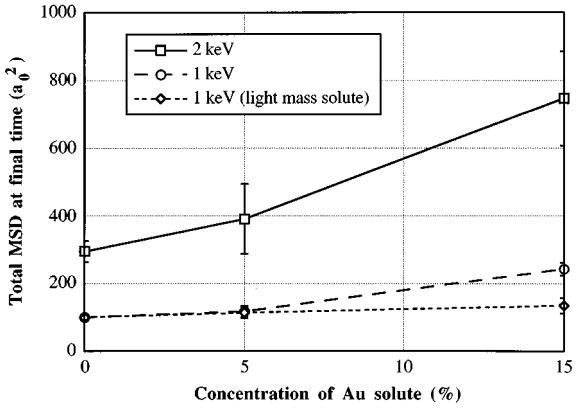

FIG. 12. Variation of the total MSD in the final state as a function of E_p and solute concentration. The data are averaged over all cascades at each condition.

The MSD data taken from the final state of all the 1- and 2-keV cascades simulated are plotted in terms of the means and standard deviations for each energy and alloy condition in Fig. 12. The contribution of the solute atoms is not identified separately, but follows the trends discussed for the individual cascades above. The information plotted emphasizes not only the nonlinear effect of cascade energy referred to above, but also the important influence of the presence of solute on atomic mixing. Solute Au atoms of normal mass increase the MSD under all conditions, with a particularly strong effect at the higher concentration. There is an inverse mass effect in the MSD for the 1-keV cascades in the 15% alloys, and this does seem to be statistically significant.

VII. DISCUSSION

Despite the recent spate of studies involving computer simulation of displacement cascades in metals—see, for example, the review in Ref. 3—the present work is, to our knowledge, the first on solid solutions. Other research on alloys has been concerned with ordered intermetallics, where disorder in the form of antisite defects rather than Frenkel pairs is the dominant result of the cascade process[12,20,21] Copper has been the most widely simulated of the pure metals,[1,2,8,18] and the Cu-Au system was chosen for the research here because of the large difference in atomic mass and size of Cu and Au. It was considered that this would emphasize solute-related features of the cascade mechanisms, and therefore, in a sense, the results obtained are rather unexpected, for it has been found that the solute atoms, whether heavy or light, have little effect on the primary state of damage at the end of the cascade event. They do have a strong influence on the ballistic and thermal spike phases, however, as shown in Secs. III and IV, and this makes the overall insensitivity of the final state to the presence of solute all the more surprising. We shall return to this below.

It could be that there actually is a solute dependence of the Frenkel defect production in our Cu-Au system, but that it is small and not revealed within the number of cascades we were able to model. It would only be possible to ascertain this by continuing the simulations to generate firmer statistics: a costly process. On the other hand, it could be that the

alloy-related effects seen in real metals after irradiation do not arise from differences in the primary damage state produced in cascades, but from the influence of solute atoms on defect transport after this stage. This is no doubt true in many cases, but there is some direct evidence that solutes affect the damage formed in cascades. Ion irradiation of thin foils can produce damage in the form of vacancy dislocation loops by collapse of cascades before the end of their thermal spike. (For reviews, see Refs. 22,23.) This vacancy component of damage can be analyzed by transmission electron microscopy (TEM) to determine the yield of loops and the production efficiency of vacancies in the cascade process. Several studies on pure metals and dilute alloys have shown that this component can be affected by even small concentrations (<1 at. %) of solute. (For a review and recent results in this area, see Ref. 24.) The well-characterized observations of Vetrano *et al.*[24] illustrate the point. In nickel alloyed with small amounts of either Al (oversized solute) or Si (undersized) and irradiated with 50-keV Kr^+ ions, both the yield and loop size change from the values for pure nickel, the form of the change depending on the solute concentration. For example, the yield increases with the addition of 0.6% Si and 0.5% Al, but then decreases for 4% Si and 5% and 7% Al. Vetrano *et al.* argue that a reasonable explanation of their results can be found in terms of solute-induced effects in both the collisional and thermal spike phases of cascades. The cascade energy used in experiments to produce visible vacancy loops is much higher than that considered here, but, nonetheless, some of the features observed here are relevant to the model of Vetrano *et al.*

The key aspect of this is that solute atoms disrupt the transfer of both energy and material away from the cascade core. These two entities are envisaged as focused collision sequences (FCS's) and replacement collision sequences (RCS's). The disruption should influence the energy density, i.e., temperature, and size of the liquidlike zone in the cascade core and affect the redistribution of atoms that leads to separation of the SIA's from the vacancies and hence to phenomena such as vacancy loop formation. The data for thermal spike size and lifetime presented in Sec. IV demonstrate very clearly the importance of Au solute atoms in affecting the transfer of kinetic energy away from the damage zone in cascade-producing conditions. We shall therefore simply comment on the separation issue here.

It is clear from the plots in Figs. 1–3 that the number of individual RCS's is reduced by the presence of solute atoms, so that at the 15% composition they make a negligible contribution to damage. Hence the mechanism of RCS disruption invoked by Vetrano *et al.* occurred in our models. However, an outcome of all the atomic-scale MD simulations of cascades reported to date is the prediction that *individual* RCS's play only a minor part in defect production under cascade conditions in pure metals. As discussed in detail by Foreman *et al.*[8] and Bacon *et al.*,[4] most SIA's seem to form by a ballistic ejection process in which regions of crystal, rather than single atomic rows, are pushed out during the collision phase and these collectively displaced chains result in SIA's when a few of them fail to return to perfect lattice positions during the subsequent relaxation. This tends to be at the edge of the highly disordered ''molten'' zone in the cascade core. If the vacant sites are sufficiently distant from these SIA's when crystalline order is restored within this zone, they remain as distinct components of the primary damage state. This process occurs in the defect visualizations for copper in Figs. 1 and 3 and has been found in other pure metals, such as α-iron[6] and α-titanium;[13] i.e., it is not a characteristic solely of the fcc structure. We conclude that although RCS disruption does occur in alloys—and this was demonstrated clearly in our previous modeling of threshold displacement events[7,9]—it is not significant in cascades because RCS's themselves are of only minor importance. (Gao and Bacon[12] have recently drawn the same conclusion from modeling of cascades in the ordered alloy Ni_3Al.) The principal effect of solute atoms is to make cascades more concentrated by disruption and shortening of the collective collision chains, and this leads to an increase in the number N_d of temporarily displaced atoms. This suggests that an energy concentration phenomenon occurs, a key feature of the model of Vetrano *et al.*, and is consistent with the kinetic energy analysis in Sec. IV.

Earlier simulations of pure metals, e.g., Refs. 6,13, have shown that the means of both the peak number of displaced atoms and the final number of stable defects increase with increasing PKA energy. The striking feature of the present simulations for 1- and 2-keV cascades is that, despite the large effect of alloy concentration on the ballistic and thermal spike phases, as measured by the number of displaced atoms, the final number of Frenkel pairs is not influenced by this change to any measurable extent (Fig. 8). This arises because the increase in $N_d(\max)$ with increasing solute concentration is effectively annulled by the density and lifetime of the thermal spike, and any expected increase in the final number of Frenkel pairs does not materialize. Simulations of other metals and alloys[4] have shown that cascades that develop a dense form with the largest number of displaced atoms in the ballistic phase end up with the smallest number of Frenkel pairs. More diffuse cascades, in contrast, are more akin to a cluster of lower-energy subcascades and, since the defect production efficiency increases with decreasing energy (see below), result in a larger number of Frenkel pairs. This illustrates the importance of the thermal spike phase in controlling defect production and suggests that the vacancy-loop effects reviewed by Vetrano *et al.*[24] result from the influence of solutes on this phase rather than on RCS disruption and solute trapping of individual SIA's.

The nature of this influence is obscure, however. In the present model, it is a mechanical effect and is only revealed at high solute concentration. In reality, much smaller changes in the solute level have been found to affect vacancy-loop yield by a cascade collapse in ion irradiated thin foils, e.g., Refs. 24,25. It is difficult to explain these observations in terms of the influence found here. Coupling between the ions and electrons in the hot cascade core may be involved, for empirical correlations by Tappin *et al.*[26] suggest that it can be important, and Kapinos and Bacon[27] have recently developed a model that shows how this coupling can account for some of the experimental findings on loop yield in alloys. These electronic effects are not included in the MD simulations performed here.

The mean number of Frenkel pairs produced per cascade for *all* the simulations at 0.25, 0.5, 1, and 2 keV was 1.42, 2,50, 4.21, and 6.83, respectively. These result in an effi-

ciency factor, as defined by Foreman *et al.*,[8] of 0.34, 0.30, 0.25, and 0.20, respectively. These factors compare with values of 0.37, 0.36, 0.32, and 0.28, respectively, presented in Fig. 13 of Ref. 8 from simulations of pure copper. Bearing in mind the small sample size, these differences may not be significant. On the other hand, they may reflect slight differences in the interatomic potentials, employed. Both were based on Finnis-Sinclair-type potentials for copper derived by Ackland and coworkers,[10,28] but they differ slightly in the modifications at small distances made by Foreman *et al.* and ourselves to make them suitable for cascade modeling. Small differences in empirical potentials are unavoidable, and the small size of the difference between the two sets of data is, in a sense, encouraging.

It was noted in Sec. V that in addition to the insensitivity of total defect production to solute addition, there is no discernible trend in interstitial clustering with composition in our data (Table II). These cluster statistics may be compared with those for pure copper in the same energy range obtained in the MD simulations of Foreman *et al.*[8] (their Fig. 10). Their numbers from 15 cascades at 1 keV are 3.0, 0.8, 0.2, and 0.1 for $1i$, $2i$, $3i$, and $4i$, respectively, and the numbers for six cascades at 2 keV are 4.0, 1.0, 0.2, 0.1, 0.4, and 0.2 for $1i$, $2i$, $3i$, $4i$, $5i$, and $6i$, respectively. Thus the propensity for SIA clustering is slightly smaller in our work. It is not clear if this is due to the lower production efficiency factor for defects (see above) or a difference in the mechanism of SIA clustering, such as might arise from differences in interstitial migration energy or cluster binding energy. We would expect the positive SIA-solute atom binding energy in our alloys to reduce SIA movement and clustering.

Although the final defect state, as measured by the number of Frenkel pairs and the extent of defect clustering, has been seen to be insensitive to the solute concentration, the analysis in Sec. VI of the atomic movements to new sites shows a strong influence. The number of atoms involved and the mean distance they jump are increased significantly by the presence of Au solute. There are two contributions to this. The first occurs by the end of the ballistic phase, when, as seen in Fig. 10, many atoms have already been displaced to positions associated with new lattice sites. This effect is enhanced by the Au atoms because although their MSD per atom is less than that of the Cu atoms, their presence generates a much larger and more concentrated zone of displaced atoms (Sec. III) by the mechanisms discussed above. The second contribution arises after the ballistic phase during the remaining lifetime of the cascade. For the 2-keV cascades described in Figs. 10 and 11, for example, the MSD per atom in pure copper arises from $0.66a_0^2$ to $0.86a_0^2$ during this period, whereas the value for the Cu–15% Au alloy increases from $0.59a_0^2$ to $1.16a_0^2$. This difference must arise from the enhancement of the thermal spike by the solute. These results clearly demonstrate the possible importance of alloying effects on all parts of cascade formation and evolution and show how they combine to affect the final outcome of the cascade process.

VIII. CONCLUSIONS

This MD study of the influence of gold solute atoms on low-energy ($\leqslant$2-keV) displacement cascades in copper at 100 K has shown that they affect the ballistic phase of cascade development by increasing its duration and increasing the number of temporarily displaced atoms. The solute also restricts focused collision sequences along atomic rows.

The mechanical relaxation and thermal spike phases that follow are similarly enhanced by the presence of the solute. At 2 keV, the combined influence of these two phases results in an oscillation in the volume of the disordered cascade core with time.

Atomic mixing in the cascade core is strongly increased by gold in solution. Most of this effect is associated with movement of the copper atoms. The contribution to the mixing from the thermal spike phase is much larger when gold solute is present.

All these effects arise because the gold atoms disrupt the transfer of energy and matter away from the cascade core. Nevertheless, the final damage state is not affected by the solute, in terms of either the number of Frenkel pairs created or their clustering.

The changes in cascade phenomena due to the gold solute are not observed in alloys containing ''Au'' with an artificially light mass. This emphasizes the importance of solute mass. Also, the changes are not significant for gold concentration up to about 5 at. %.

These results have been discussed in the context that dilute concentrations of some solutes are known to affect the yield of vacancy loops in ion-irradiated metals. Since enhancement of the energy density and lifetime of the thermal spike was only found here for the combination of high solute mass and concentration, contrary to the conditions in the experiments, it would seem that the influence of solute atoms on loop yield in real alloys is not of a purely mechanical nature.

ACKNOWLEDGMENTS

This work was supported by a research grant and provision of supercomputer resources from the Engineering and Physical Sciences Research Council (EPSRC). The authors also acknowledge helpful discussions with their colleagues Andrew Calder, Gao Fei, Victor Kapinos, and Stephen Wooding.

*Present address: Department of Engineering, Queen Mary and Westfield College, Mile End Road, London E1 4NS, United Kingdom.

[1] T. Diaz de la Rubia and M. W. Guinan, Mater. Sci. Forum **97-99**, 23 (1992).

[2] T. Diaz de la Rubia and W. J. Phythian, J. Nucl. Mater. **191-194**, 108 (1992).

[3] D. J. Bacon and T. Diaz de la Rubia, J. Nucl. Mater. **216**, 275 (1994).

[4] D. J. Bacon, A. F. Calder, F. Gao, V. G. Kapinos, and S. J. Wooding, Nucl. Instrum. Methods Phys. Res. B **102**, 37 (1995).

[5] M. W. Finnis (unpublished).

[6] A. F. Calder and D.J. Bacon, J. Nucl. Mater. **207**, 25 (1993).

[7] H. F. Deng and D. J. Bacon, Phys. Rev. B **48**, 10 022 (1993).

[8] A. J. E. Foreman, W. J. Phythian, and C. A. English, Philos. Mag. A **66**, 671 (1992).
[9] H. F. Deng and D. J. Bacon, Radiat. Eff. Defects Solids **130-131**, 507 (1994).
[10] G. J. Ackland and V. Vitek, Phys. Rev. B **41**, 10 324 (1990).
[11] D. J. Bacon, H. F. Deng, and F. Gao, J. Nucl. Mater. **205**, 84 (1993).
[12] F. Gao and D. J. Bacon, Philos. Mag. A **71**, 43 (1995).
[13] S. J. Wooding, D. J. Bacon, and W. J. Phythian, Philos. Mag. A **72**, 1261 (1995).
[14] F. Gao and D. J. Bacon (unpublished).
[15] V. G. Kapinos and D. J. Bacon, Phys. Rev. B **50**, 13 194 (1994).
[16] C. H. Woo and B. N. Singh, Philos. Mag. A **65**, 889 (1992).
[17] S. J. Zinkle and B. N. Singh, J. Nucl. Mater. **199**, 173 (1993).
[18] T. Diaz de la Rubia, R. S. Averback, H. Hsieh, and R. Benedek, J. Mater. Res. **4**, 579 (1989).
[19] R. S. Averback, J. Nucl. Mater. **216**, 49 (1994).
[20] T. Diaz de la Rubia, A. Caro, and M. Spaczer, Phys. Rev. B **47**, 11 483 (1993).
[21] H. Zhu, R. S. Averback, and M. Nastasi, Philos. Mag. A **71**, 735, (1995).
[22] C. A. English and M. L. Jenkins, Mater. Sci. Forum **15-18**, 1003 (1987).
[23] C. A. English, A. J. E. Foreman, W. J. Phythian, D. J. Bacon, and M. L. Jenkins, Mater. Sci. Forum **97-99**, 1 (1992).
[24] J. S. Vetrano, I. M. Robertson, and M. A. Kirk, Philos. Mag. A **68**, 381 (1993).
[25] A. Y. Stathopoulos, C. A. English, B. L. Eyre, and P. B. Hirsch, Philos. Mag. A **44**, 309 (1981).
[26] D. K. Tappin, I. M. Robertson, and M. A. Kirk, Philos. Mag. A **70**, 463 (1994).
[27] V. G. Kapinos and D. J. Bacon, Phys. Rev. B **52**, 4029 (1995).
[28] G. J. Ackland, G. Tichy, V. Vitek, and M. W. Finnis, Philos. Mag. A **56**, 735 (1987).
[29] W. E. King, K. L. Merkle, and M. Meshii, J. Nucl. Mater. **117**, 12 (1983).